JOURNAL OF COMPUTATIONAL PHYSICS 50, 482–498 (1983)

# Numerical Solution of the Zakharov Equations*

G. L. PAYNE, D. R. NICHOLSON, AND R. M. DOWNIE

*Department of Physics and Astronomy, The University of Iowa, Iowa City, Iowa 52242*

Received February 23, 1982; revised September 23, 1982

A new algorithm for the numerical solution of the Zakharov equations is presented. This algorithm is explicit and it is second-order accurate. The convergence of the algorithm is demonstrated by numerically solving the Zakharov equations for several test cases.

## 1. INTRODUCTION

One of the most fundamental and fascinating phenomena in plasma physics is Langmuir turbulence [1, 2]. Although in the low-amplitude linear limit this turbulence consists only of high-frequency electron oscillations, the presence of larger amplitude waves induces nonlinearities which couple the high-frequency electron oscillations to low-frequency ion oscillations. These nonlinearities lead to parametric instabilities, including a three-wave interaction called the parametric decay instability and a four-wave interaction called the modulational instability or oscillating two-stream instability [3]. The strongly nonlinear state leads to the formation of coherent structures called solitons [4]; these structures are stable in one dimension and can collapse catastrophically in two or three dimensions [5–9]. Zakharov [5] (see also Hasegawa [10]) introduced a relatively simple set of fluid equations to describe all of these physical phenomena. In one spatial dimension, the Zakharov equations are

$$i\,\partial_t E(x,t) + \partial_x^2 E = nE, \tag{1}$$

$$\partial_t^2 n(x,t) - \partial_x^2 n = \partial_x^2 |E|^2, \tag{2}$$

where $t$ is dimensionless time, $x$ is dimensionless distance, $E(x, t)$ is the dimensionless slowly varying envelope of the high-frequency electric field, and $n(x, t)$ is the dimensionless low-frequency density variation. The numerical and analytic study of the properties of (1) and (2) is a very active area of research in fundamental plasma physics [5–13].

We are interested in solutions of the Zakharov equations for periodic systems with a large enough period so that the length of the individual solitons is small compared

* This work was supported by the National Science Foundation, Atmospheric Research Section, ATM81-15396 and ATM81-11126, USDOE DE-AC02-82ER53136, and NASA NSG-7632. Part of this research was performed while Mr. Nicholson was a guest of the Aspen Center for Physics.



0021-9991/83 $3.00

Copyright © 1983 by Academic Press, Inc.
All rights of reproduction in any form reserved.

to the period. A standard technique to obtain accurate representations of the spatial variations is to use the spectral method [14]. In this method we solve in the time variable by a finite difference method. Since the algorithm should provide accurate answers at asymptotic times, it is necessary to use many small time steps. Thus, we would like to have a stable, efficient, and accurate algorithm for time integration. Normally, for nonlinear differential equations the numerical algorithm leads to nonlinear equations which must be solved by iteration; that is, the method is an implicit scheme [14, 15]. As many as 10 iterations are required to solve these implicit schemes [15]. Since these iterations require a considerable amount of computer time, we present in this paper an algorithm which is explicit and is second-order accurate (the local error is proportional to the time step cubed). In Section 2 we derive the algorithm and in Section 3 we find an analytic solution of the Zakharov equations for the periodic case. In Section 4 we test the algorithm for this analytic solution and for a more realistic case which does not have an analytic solution. The method is shown to be accurate, stable, and efficient.

## 2. Derivation of Algorithm

For a periodic system an accurate and efficient numerical method for the solution of the spatial dependence is the spectral method using the fast Fourier transform [16]. The time evolution of the system is followed by numerically integrating the equations for the time variation of the Fourier components. In the spectral method the spatial derivatives and integrals can be evaluated exactly for a given representation. Using the fast Fourier transform yields convolution sums in the Fourier space for the nonlinear terms in Eqs. (1) and (2). These convolution sums can be performed efficiently by transforming back to configuration space, performing the local products, and then taking the fast Fourier transform of the products. In the last step of this procedure, additional terms can appear because of the truncation of the Fourier expansion; these terms are called aliasing terms. It has been shown [17–19] that for nonlinear equations these aliasing terms can introduce errors which grow in time. For quadratic nonlinearities of the type found in the one-dimensional Zakharov equations, the aliasing terms can be eliminated by using only two-thirds of the Fourier components for a particular mesh in the fast Fourier transform.

For a system with a period $L$, we define the set of $N$ grid points $x_j$ in configuration space by

$$x_j = \frac{jL}{N}, \tag{3}$$

for $j = 0, 1, 2, \ldots, N-1$. Then the discrete Fourier representations of $E(x, t)$ and $n(x, t)$ are given by

$$E(x_j, t) = E_j(t) = \sum_{k=-K}^{K} E_k(t)\, e^{ikx_j}, \tag{4}$$

and

$$n(x_j, t) = n_j(t) = \sum_{k=-K}^{K} n_k(t)\, e^{ikx_j}. \tag{5}$$

In (4) and (5) the sums are over the values

$$k = \frac{2\pi m}{L}, \qquad -M \leqslant m \leqslant M,$$

where we choose $M < N/3$ to eliminate the aliasing terms and where $K = 2\pi M/L$. Thus, we use a truncated Fourier expansion.

Substituting (4) and (5) into Eqs. (1) and (2), we obtain the set of ordinary differential equations for the Fourier components

$$\partial_t E_k + v_e E_k + ik^2 E_k = -i(nE)_k, \tag{6}$$

$$\partial_t^2 n_k + 2v_i\, \partial_t n_k + k^2 n_k = -k^2(|E|^2)_k, \tag{7}$$

where we have included the damping terms which appear in more realistic cases. In all of the results presented in this paper, $v_e = v_i = 0$. Nevertheless, we shall carry these terms through the derivation in order to obtain the more general algorithm. We assume that the damping coefficients are linear; that is, they do not depend upon $E_k$ or $n_k$. These damping coefficients may be functions of $k$.

Using standard techniques [20], we rewrite Eqs. (6) and (7) as the integral equations

$$\begin{aligned} n_k(t) = {} & n_k(0) \exp(-v_i t) \left[\cos(\sqrt{k^2 - v_i^2}\, t) + v_i \frac{\sin(\sqrt{k^2 - v_i^2}\, t)}{\sqrt{k^2 - v_i^2}}\right] \\ & + n_k'(0) \exp(-v_i t) \frac{\sin(\sqrt{k^2 - v_i^2}\, t)}{\sqrt{k^2 - v_i^2}} \\ & - k^2 \int_0^t (|E^2|)_k \exp[-v_i(t - t')] \frac{\sin[\sqrt{k^2 - v_i^2}\, (t - t')]}{\sqrt{k^2 - v_i^2}}\, dt' \end{aligned} \tag{8}$$

and

$$\begin{aligned} E_k(t) = {} & E_k(0) \exp[-(ik^2 + v_e)t] \\ & - i \int_0^t (nE)_k \exp[-(ik^2 + v_e)(t - t')]\, dt', \end{aligned} \tag{9}$$

where $n_k'$ is the first derivative of $n_k$ with respect to time.

Setting $t = h$, and using the trapezoidal rule to approximate the integrals, we find

$$n_k(h) = n_k(0)\exp(-v_i h)\left[\cos(\sqrt{k^2 - v_i^2}\,h) + v_i\frac{\sin(\sqrt{k^2 - v_i^2}\,h)}{\sqrt{k^2 - v_i^2}}\right]$$
$$+ n_k'(0)\exp(-v_i h)\frac{\sin(\sqrt{k^2 - v_i^2}\,h)}{\sqrt{k^2 - v_i^2}}$$
$$- \left(\frac{h}{2}\right)k^2(|E(0)|^2)_k\exp(-v_i h)\frac{\sin(\sqrt{k^2 - v_i^2}\,h)}{\sqrt{k^2 - v_i^2}} + O(h^3) \tag{10}$$

and

$$E_k(h) = E_k(0)\exp[-(ik^2 + v_e)h] - i(h/2)\{[n(h)\,E(h)]_k$$
$$+ [n(0)\,E(0)]_k\exp[-(ik^2 + v_e)h]\} + O(h^3). \tag{11}$$

In these equations $n$ and $E$ with no subscripts represent the configuration space expressions $n(x, t)$ and $E(x, t)$.

Equation (10) provides a value for $n_k(h)$ in terms of $n_k(0)$, $n_k'(0)$, and $E(0)$. Given the value $n_k(0)$, we can find $n(h)$, then Eq. (11) can be solved for $E(h)$. As mentioned, the convolution sums $(nE)_k$ and $(|E|^2)_k$ can be evaluated by using the fast Fourier transform. To solve Eq. (11) we first evaluate

$$\tilde{E}_k = E_k(0)\exp[-(ik^2 + v_e)h] \tag{12}$$

and

$$(\widetilde{nE})_k = [n(0)\,E(0)]_k\exp[-(ik^2 + v_e)h]. \tag{13}$$

Then taking the inverse Fourier transform of Eq. (11), we find

$$E_j(h) = \tilde{E}_j - i(h/2)[n_j(h)\,E_j(h) + (\widetilde{nE})_j]. \tag{14}$$

Since $n_j(h)$ is given by the solution to Eq. (10), Eq. (14) can be used to find $E_j(h)$. The result is

$$E_j(h) = \frac{\tilde{E}_j - i(h/2)(\widetilde{nE})_j}{1 + i(h/2)\,n_j(h)}. \tag{15}$$

Finally, the fast Fourier transform can be used to find $E_k(h)$. Thus, the equations have been advanced one time step and the error is proportional to $h^3$. From this derivation we can see that the reasons for obtaining an explicit scheme are that Eq. (2) is a Helmholtz equation, and Eq. (1) is linear in the electric field $E$.

In order to continue the integration in time, we need the value of $n_k'(h)$. Given the value of $n$ and $E$, we can determine the value of $n'$. To show this we define

$$v_k \equiv n_k' \tag{16}$$

and rewrite Eq. (7) in the form

$$\partial_t v_k + 2v_i v_k = -k^2 n_k - k^2(|E|^2)_k. \tag{17}$$

This equation can be rewritten as the integral equation

$$v_k(t) = v_k(0)\exp(-2v_i t) - k^2 \int_0^t [n_k + (|E|^2)_k] \times \exp[-2v_i(t-t')]\, dt'. \tag{18}$$

Setting $t = h$ and using the trapezoidal rule to approximate the integral, we find

$$n_k'(h) = n_k'(0)\exp(-2v_i h) - (h/2)\, k^2 \{[n_k(0) + (|E(0)|^2)_k] \times \exp(-2v_i h) + n_k(h) + (|E(h)|^2)_k\} + O(h^3). \tag{19}$$

Thus, Eqs. (10), (15), and (19) can be used to advance the solution of the Zakharov equations one time step. The algorithm is explicit and it is second-order accurate (i.e., the error is proportional to $h^3$). In Section 4 we use the algorithm to solve the Zakharov equations for several test cases. The numerical results demonstrate the stability and convergence rate of the algorithm.

## 3. Analytic Solution

An analytic solution of the Zakharov equations can be found by using the energy method [21]. To find this solution we assume the forms

$$E(x, t) = F(x - vt)\exp[i\varphi(x - ut)] \tag{20}$$

and

$$n(x, t) = G(x - vt). \tag{21}$$

Substituting these forms into Eq. (2), we find for the periodic system that

$$G(x - vt) = -\frac{|F(x - vt)|^2}{1 - v^2} + n_0, \tag{22}$$

where the constant of integration $n_0$ is chosen so that

$$\langle n \rangle = \frac{1}{L}\int_0^L n(x, t)\, dx = 0. \tag{23}$$

Substituting the expressions (20) and (21) into Eq. (1) gives

$$\varphi = \frac{v}{2} \tag{24}$$

and

$$F'' = \left(\frac{v^2}{4} - \frac{vu}{2} + n_0\right) F - \frac{F^3}{1 - v^2}, \tag{25}$$

where $F''$ means the second derivative with respect to the argument. The solution to Eq. (25) is

$$F(x - vt) = E_{\max}\, dn(w, q), \tag{26}$$

where $dn(w, q)$ is a Jacobian elliptic function [22, 23]

$$w = \left[\frac{E_{\max}}{\sqrt{2(1 - v^2)}}\right](x - vt) \tag{27}$$

and

$$q = \frac{\sqrt{E_{\max}^2 - E_{\min}^2}}{E_{\max}}. \tag{28}$$

The two constants of integration $E_{\max}$ and $E_{\min}$ are the maximum and minimum values of the electric field, respectively. In order that (26) satisfies Eq. (25), the constant $u$ must have the value

$$u = \frac{v}{2} + \frac{2n_0}{v} - \frac{(E_{\max}^2 + E_{\min}^2)}{v(1 - v^2)}. \tag{29}$$

The period of the Jacobian elliptic functions is given by

$$L = \frac{2\sqrt{2(1 - v^2)}}{E_{\max}} K(q) = \frac{2\sqrt{2(1 - v^2)}}{E_{\max}} K'\left(\frac{E_{\min}}{E_{\max}}\right), \tag{30}$$

where $K$ and $K'$ are complete elliptic integrals of the first kind [22, 23] and we have used $K(q) = K'(\sqrt{1 - q^2})$. For a periodic solution the exponential term in (20) must also have a period equal to $L$; thus, we require

$$\frac{v}{2} L = 2\pi m, \qquad m = 1, 2, 3, \ldots. \tag{31}$$

For the test cases given in the next section, the value of $m$ was chosen to be one.

As $E_{\min} \to 0$ the parameter $q \to 1$ and the period of the elliptic functions becomes infinite. For $q = 1$,

$$dn(w, 1) = \operatorname{sech} w \tag{32}$$

and for an infinite period the value of $n_0$ is zero. Therefore, for the infinite period case, the solution reduces to the usual hyperbolic secant form [24].

The procedure for obtaining a periodic analytic solution is to: (1) choose values for $E_{max}$ and $L$; (2) determine $v$ from Eq. (31); and (3) find a value of $E_{min}$ such that Eq. (30) is satisfied. In the next section we give the values of the parameters for two solutions with a period $L = 20$ and one solution with a period $L = 160$.

## 4. Numerical Results

For the first test cases of the algorithm we choose two solutions for a system with a period of 20.0 units. The first case has $E_{max} = 1.0$ and the second case has $E_{max} = 10.0$. The values of the various parameters for these two cases are given in Table I. In Fig. 1 we plot the absolute value of the electric fields at $t = 0$ for these two cases. From Table I it is obvious that the $E_{max} = 10.0$ case will require a much smaller time step for convergence than the $E_{max} = 1.0$ case, since the phase speed $u$ of the electric field is much larger for $E_{max} = 10.0$.

To demonstrate the convergence of the algorithm, we start at $t = 0$ and integrate the equations until the soliton has moved a fixed distance $D$. Since the number of time steps is proportional to $h^{-1}$, the global error should be proportional to $h^2$ if the error for each time step is of order $h^3$. We define the error $\varepsilon$ as

$$\varepsilon = \left[ \int_0^L |E(x,t) - E_h(x,t)|^2 \, dx \Big/ \int_0^L |E(x,t)|^2 \, dx \right]^{1/2}, \tag{33}$$

where $E(x, t)$ is the analytic solution and $E_h(x, t)$ is the numerical solution. In order to obtain accurate solutions of Eqs. (1) and (2) it is necessary that the number of Fourier components in Eqs. (4) and (5) be large enough to accurately represent the solution at any instant of time. In Fig. 2 we show the error in the expansion at $t = 0$ for various values of $M$. Since we are interested in the error caused by the time step, we must choose $M$ large enough so that the initial error is much smaller than the error from the finite size of $h$. For the $E_{max} = 1.0$ case we use $M = 21$ ($N = 64$) and $M = 42$ ($N = 128$). For the $E_{max} = 10.0$ case we use $M = 170$ ($N = 512$). For these values of $M$ the error of the initial fit to the analytic expression is much smaller than the errors from the time integration.

TABLE I

Parameters for Three Analytic Solutions of the Periodic Zakharov Equations

| | $L$ | $E_{max}$ | $E_{min}$ | $v$ | $u$ | $n_0$ |
|---|---|---|---|---|---|---|
| $A$ | 20.0 | 1.0 | $4.5147 \times 10^{-4}$ | 0.628319 | −1.73692 | 0.181786 |
| $B$ | 20.0 | 10.0 | $1.3421 \times 10^{-38}$ | 0.628319 | −256.872 | 1.81786 |
| $C$ | 160.0 | 1.0 | $1.0535 \times 10^{-31}$ | ±0.628319 | ∓2.24323 | 0.0227232 |

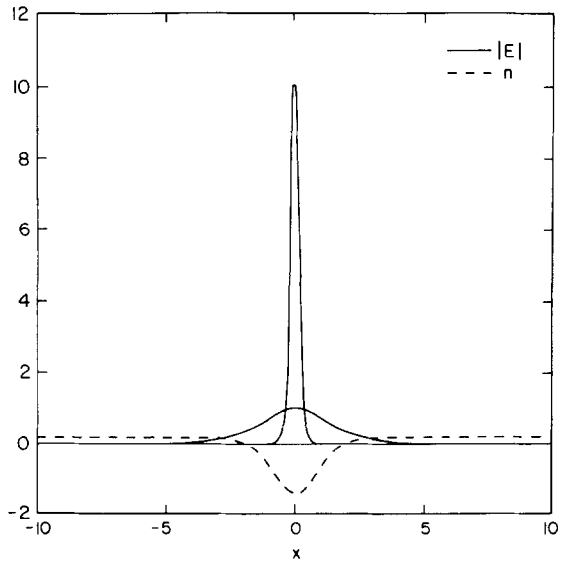


FIG. 1. Absolute value of the electric field at $t = 0$ for $E_{max} = 1.0$ and $E_{max} = 10.0$. Also shown is the value of $n$ at $t = 0$ for the $E_{max} = 1.0$ case.

As an additional test of the convergence, we evaluate the values of the conserved quantities [24]

$$N = \int_0^L |E|^2 \, dx, \tag{34}$$

$$P = \int_0^L \left[ \frac{i}{2} (E \, \partial_x E^* - E^* \, \partial_x E) + nV \right] dx, \tag{35}$$

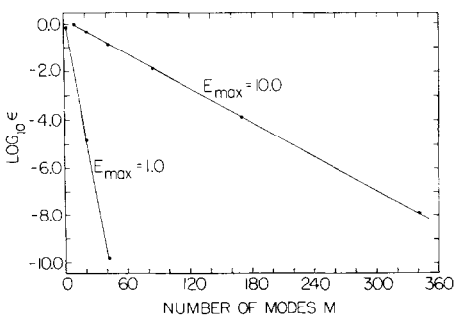


FIG. 2. Error in the Fourier expansion of $E(x, t)$ at $t = 0$.

and

$$H = \int_0^L [|\partial_x E|^2 + n|E|^2 + \tfrac{1}{2}n^2 + \tfrac{1}{2}V^2]\, dx, \tag{36}$$

where $V$ is the flux. The value of $V$ is determined from the continuity equation,

$$\partial_t n + \partial_x V = 0. \tag{37}$$

For the $E_{\max} = 1.0$ case we choose $D = 20.0$; that is, we integrate the equations until the soliton has moved through one period. In Table II we show the values of $\varepsilon$ for various step sizes for $M = 21$ ($N = 64$). Also, the values of the conserved quantities are given. From this table one can see that the values of the conserved quantities converge much more rapidly than the value of the solution. This demonstrates that the values of the conserved quantities are not necessarily a good test of the convergence of the solution [18, 19]. In Table III we give some representative values of the error for $M = 42$ ($N = 128$). Once the solution starts to converge, the errors are the same for $M = 21$ and $M = 42$. In Fig. 3 we plot the error as a function of the step size $h$. The slope of the straight line drawn through the points is two. Thus, we find that the error is proportional to $h^2$ as predicted.

TABLE II

Values of the Error and the Conserved Quantities for Various Values of the Time Step Size $h$ for $E_{\max} = 1.0$ ($M = 21, N = 64$)

| $h$ | $\varepsilon$ | $N$ | $P$ | $H$ |
|---|---|---|---|---|
| 0.15915 | 0.7694 | 2.1909860 | 1.9193250 | 1.1581687 |
| 0.14469 | 0.2454 | 2.2007159 | 2.7777824 | 1.1385435 |
| 0.13263 | 0.2055 | 2.2006243 | 2.7812398 | 1.1337540 |
| 0.11368 | 0.1496 | 2.2005242 | 2.7852713 | 1.1271708 |
| 0.09947 | 0.1138 | 2.2004703 | 2.7875208 | 1.1284796 |
| 0.08377 | 0.0800 | 2.2004327 | 2.7894125 | 1.1295930 |
| 0.07958 | 0.0720 | 2.2004257 | 2.7898196 | 1.1298345 |
| 0.06366 | 0.0455 | 2.2004078 | 2.7910314 | 1.1305581 |
| 0.05305 | 0.0313 | 2.2004015 | 2.7915768 | 1.1308869 |
| 0.04547 | 0.0228 | 2.2003989 | 2.7918571 | 1.1310570 |
| 0.03979 | 0.0174 | 2.2003976 | 2.7920155 | 1.1311536 |
| 0.03183 | 0.0110 | 2.2003967 | 2.7921734 | 1.1312503 |
| 0.02653 | 0.0076 | 2.2003963 | 2.7922435 | 1.1312934 |
| 0.02274 | 0.0056 | 2.2003962 | 2.7922793 | 1.1313155 |
| 0.01989 | 0.0042 | 2.2003962 | 2.7922995 | 1.1313279 |
| 0.01592 | 0.0027 | 2.2003962 | 2.7923195 | 1.1313403 |
| 0.01326 | 0.0019 | 2.2003962 | 2.7923284 | 1.1313458 |
| 0.01137 | 0.0014 | 2.2003962 | 2.7923330 | 1.1313487 |
| 0.00995 | 0.0010 | 2.2003962 | 2.7923355 | 1.1313502 |
| Initial | | 2.2003964 | 2.7923410 | 1.1313535 |

TABLE III

Values of the Error and the Conserved Quantities for Various Values of the Time Step Size $h$ for $E_{max} = 1.0$ ($M = 42, N = 128$)

| $h$ | $\varepsilon$ | $N$ | $P$ | $H$ |
|---|---|---|---|---|
| 0.15915 | 0.3871 | 2.2011965 | 2.6708686 | 3.4969320 |
| 0.07958 | 0.0719 | 2.2004262 | 2.7898209 | 1.1298360 |
| 0.03979 | 0.0174 | 2.2003981 | 2.7920166 | 1.1311539 |
| 0.01989 | 0.0042 | 2.2003965 | 2.7923001 | 1.1313281 |
| Initial | | 2.2003964 | 2.7923410 | 1.1313535 |

For the $E_{max} = 10.0$ case we choose $D = 1.0$. For this case a much smaller time step is required for convergence, and in order to reduce the amount of computer time we have chosen a smaller value of $D$ for this case. In Table IV we give the value of $\varepsilon$ for various values of $h$, as well as the values of the conserved quantities. Once again, we find that the values of the conserved quantities converge much more rapidly than the value of the solution. In Fig. 4 we plot the error as a function of $h$ and we find that the error is proportional to $h^2$. The much smaller value of $h$ required to obtain an accurate solution is to be expected since we have used the trapezoidal rule to integrate the nonlinear terms; for larger values of $E$ and $n$ the nonlinear terms will be larger and a smaller value of $h$ will be required to give accurate numerical results. For $E_{max} = 10.0$ the nonlinear terms are $10^3$ times the nonlinear terms for $E_{max} = 1.0$ and the ratio of the step sizes required in order to obtain the same value of $\varepsilon$ is $3 \times 10^{-3}$. Thus, we see that the step size required for an accurate solution depends upon the values of $E$ and $n$ for the particular case being studied.

Finally, as a more realistic test of the algorithm we consider the case of two colliding solitons. For this case we consider two solutions with the same value of $E_{max} = 1.0$ but with oppositely directed velocities. In order to study the effects of the collision we consider a much longer system. We have chosen $L = 160.0$ so that the waves emitted by the collision stay within the system during the time period of the

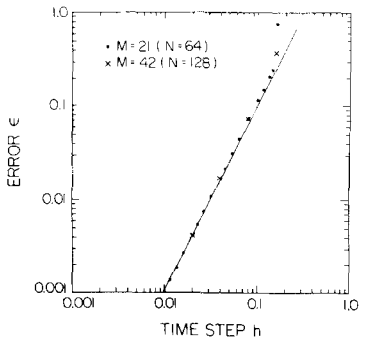


FIG. 3. Error in $E(x, t)$ as a function of the step size $h$ for $E_{max} = 1.0$ ($D = 20.0$). The straight line has been drawn with a slope of 2.0 through the bottom point to show that the global error goes as $h^2$.

TABLE IV

Values of the Error and the Conserved Quantities for Various Values of the Time Step Size $h$ for $E_{max} = 10.0$ ($M = 170, N = 512$)

| $h$ | $\varepsilon$ | $N$ | $P$ | $H$ |
|---|---|---|---|---|
| 0.001273 | 0.8980 | 22.006015 | 2481.7097 | 971.89067 |
| 0.001061 | 0.6423 | 22.004228 | 2481.7110 | 971.58963 |
| 0.000796 | 0.3704 | 22.003139 | 2481.7124 | 971.38565 |
| 0.000637 | 0.2397 | 22.002947 | 2481.7133 | 971.32040 |
| 0.000455 | 0.1238 | 22.003025 | 2481.7142 | 971.27270 |
| 0.000318 | 0.0615 | 22.003227 | 2481.7149 | 971.24553 |
| 0.000159 | 0.0162 | 22.003553 | 2481.7157 | 971.21623 |
| 0.000106 | 0.0077 | 22.003674 | 2481.7160 | 971.20641 |
| Initial | | 22.003923 | 2481.7166 | 971.18653 |

computer run. The parameters for the two solitons are given in Table I. In Fig. 5 we show the real and imaginary parts of the electric field at $t = 0$.

Since the solution for two colliding solitons cannot be written in an analytic form we have chosen an extremely accurate numerical solution to use as the exact result in Eq. (33) for the error $\varepsilon$. Using this "exact" solution we show in Fig. 6 the value of the error as a function of $h$ for two different times. The time $t = 15.9$ corresponds to the time when the two solitons are at the same position and the time $t = 31.8$ corresponds to a time when the collision is nearing completion. For both times we find the error is proportional to $h^2$ as predicted.

To show the effects of the collision, we have plotted in Figs. 7 and 8 the values of $|E(x, t)|$ and $n(x, t)$ at various times. From these plots we can see that during the collision waves are emitted, and that after the collision the two solitons have a

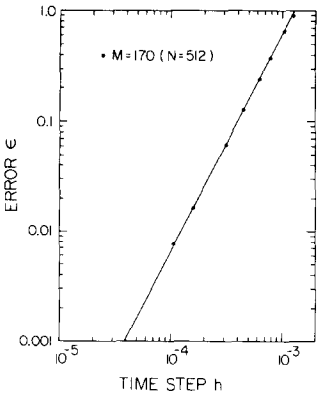


FIG. 4. Error in $E(x, t)$ as a function of the step size $h$ for $E_{max} = 1.0$ ($D = 1.0$). The straight line has been drawn with a slope of 2.0 through the bottom point to show that the global error goes as $h^2$.

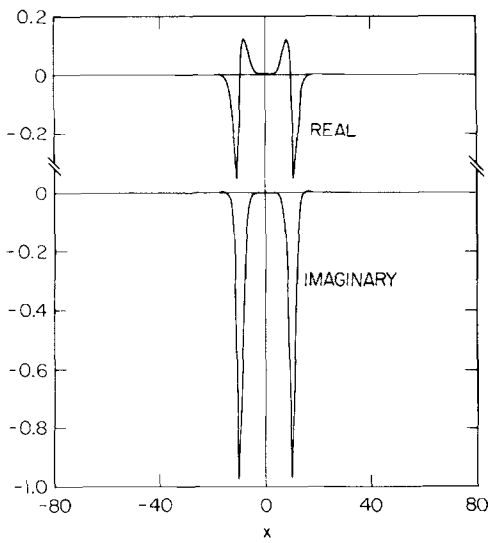


FIG. 5. Real and imaginary components of the electric field at $t = 0$ for two solitons with $E_{max} = 1.0$. Each soliton is moving with a speed $v$ towards the origin.

reduced value of $E_{max}$. The density waves move at the sound speed, and the electric field waves move more rapidly. In Figs. 9 and 10 we show the values of the electric field and the density at $t = 31.8$.

Since the values of $E$ and $n$ are much larger during the collision, we expect that the errors will be larger during this time. To demonstrate that this is the case, we have

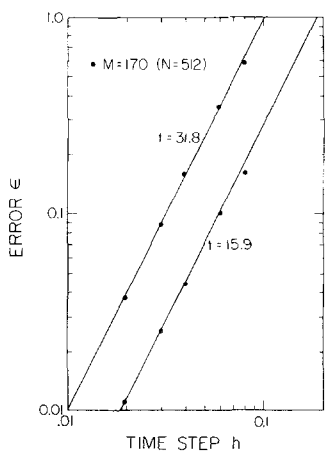


FIG. 6. Error in $E(x, t)$ as a function of the step size $h$ for two colliding solitons. The straight line has been drawn with a slope of 2.0 to show that the global error goes as $h^2$.

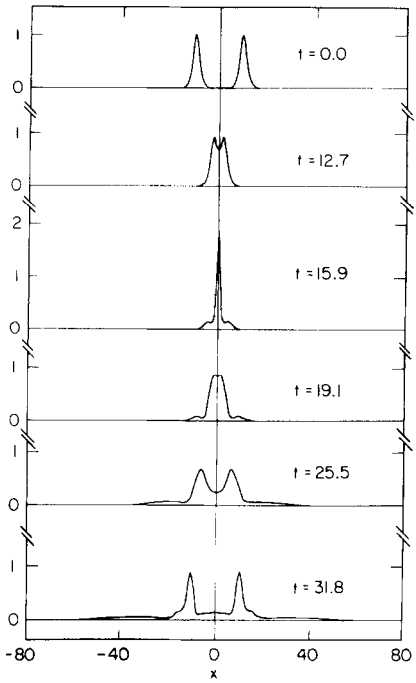


FIG. 7. Absolute value of the electric field for various times for two colliding solitons with $E_{max} = 1.0$.

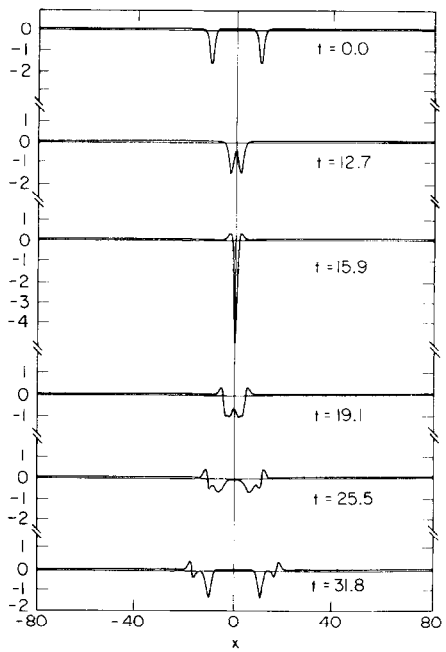


FIG. 8. The density for various times for the two colliding solitons shown in Fig. 7.

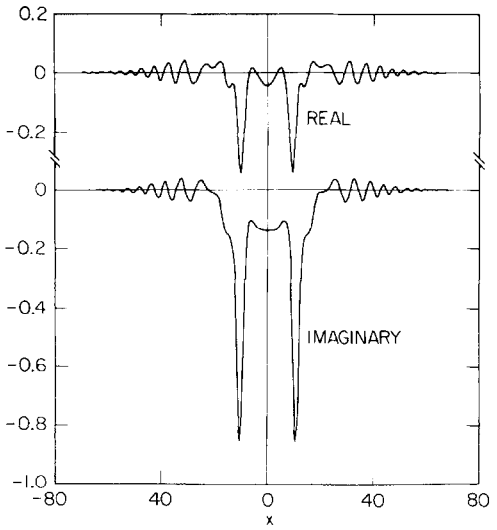


FIG. 9. The real and imaginary components of the electric field at $t = 31.8$ for two colliding solitons.

plotted the errors in the conserved quantities $N$ and $H$ as a function of time in Figs. 11 and 12. We have defined the errors as

$$\varepsilon_N = \frac{N - N_n(t)}{N} \quad \text{and} \quad \varepsilon_H = \frac{H - H_n(t)}{H},$$

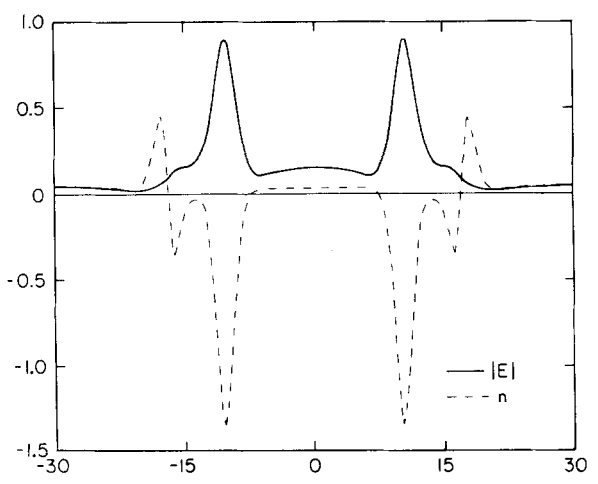


FIG. 10. The absolute value of the electric field and the density at $t = 31.8$ for two colliding solitons.

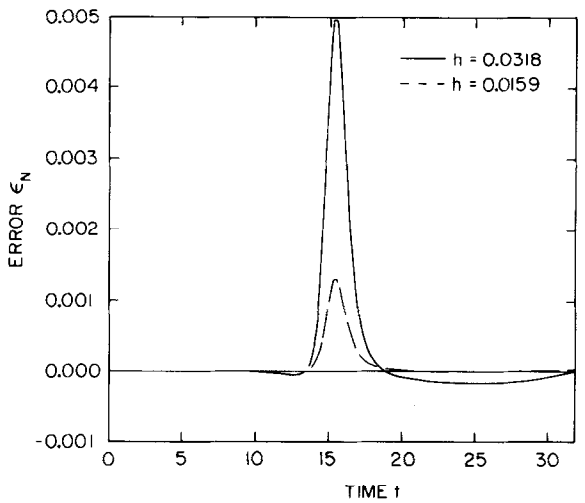


FIG. 11. Error in the conserved quantity $N$ as a function of time for two different values of the step size $h$.

where $N$ and $H$ are the initial values of the conserved quantities, and $N_n(t)$ and $H_n(t)$ are the values of the conserved quantities at time $t$ evaluated using the numerical solution of the equation found with a step size $h$. From Figs. 11 and 12 we can see that during the collision, which occurs around the time $t = 15.9$, the errors in the conserved quantities are much larger. The errors in these conserved quantities decrease after the collision. During the collision larger values of $k$ are important and

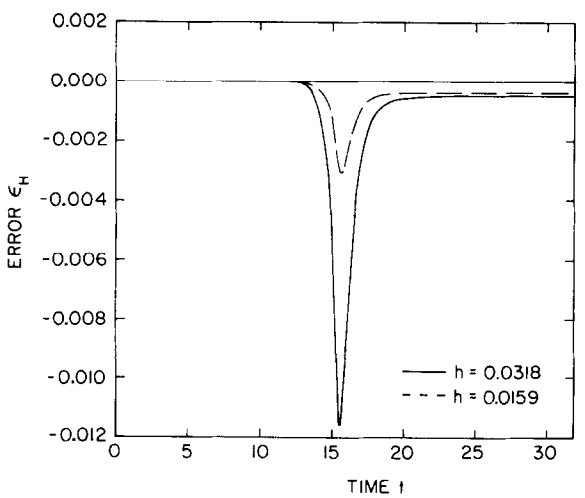


FIG. 12. Error in the conserved quantity $H$ as a function of time for two different values of the step size $h$.

a smaller step size is required to accurately advance these modes. After the collision these modes are not as important and the numerical errors in these modes have a smaller effect on the values of $N$ and $H$.

Although it is not the purpose of this paper to present a detailed physical discussion of the collision of two Langmuir solitons, we do note the presence of nonsolitonic radiation in the density $n$ (Fig. 8 at times 25.5 and 31.8) and in the electric field $E$ (Fig. 9). This radiation is a significant feature of the collision of two solitons in a nonintegrable system [25] and analytic descriptions are available [26]. The shelf-like structures seen most vividly in $|E|$ around $x = \pm 15$ in Fig. 10 have seen a great deal of study in connection with soliton propagation in density gradients and in dissipative media [27, 28].

## ACKNOWLEDGMENTS

We thank B. Hafizi, G. Knorr, H. A. Rose, and especially G. R. Joyce for useful discussions, and G. D. Doolen for supplying one of the data points. We are grateful to the referee for several useful suggestions.

## REFERENCES

1. I. LANGMUIR, *Proc. Natl. Acad. Sci. U.S.A.* **14** (1926), 627.
2. L. TONKS AND I. LANGMUIR, *Phys. Rev.* **33** (1929), 195.
3. F. F. CHEN, "Introduction to Plasma Physics," Plenum, New York, 1974.
4. A. C. SCOTT, F. Y. F. CHU, AND D. W. MCGLAUGHLIN, *Proc. IEEE* **61** (1973), 1443.
5. V. E. ZAKHAROV, *Zh. Eksp. Teor. Fiz.* **62** (1972), 1745; *Sov. Phys.-JETP* **35** (1972), 908.
6. N. R. PEREIRA, R. N. SUDAN, AND J. DENAVIT, *Phys. Fluids* **20** (1977), 936.
7. D. R. NICHOLSON, M. V. GOLDMAN, P. HOYNG, AND J. C. WEATHERALL, *Astrophys. J.* **223** (1978), 605.
8. M. V. GOLDMAN AND D. R. NICHOLSON, *Phys. Rev. Lett.* **41** (1978), 406.
9. D. R. NICHOLSON AND M. V. GOLDMAN, *Phys. Fluids* **21** (1978), 1766.
10. A. HASEGAWA, *Phys. Rev.* **1A** (1970), 1746.
11. A. THYAGARAJA, *Phys. Fluids* **24** (1981), 1973.
12. D. A. RUSSELL AND E. OTT, *Phys. Fluids* **24** (1981), 1976.
13. J. C. WEATHERALL, J. P. SHEERIN, D. R. NICHOLSON, G. L. PAYNE, M. V. GOLDMAN, AND P. J. HANSEN, *J. Geophys. Res.* **87** (1982), 823.
14. F. TAPPERT, *Lect. Appl. Math.* **15** (1974), 215.
15. L. M. DEGTYAREV, *Sov. Phys.-Dokl.* **24** (1979), 716.
16. D. GOTTLIEB AND S. A. ORSZAG, "Numerical Analysis of Spectral Methods," SIAM, Philadelphia, 1977.
17. S. A. ORSZAG, *J. Fluid Mech.* **49** (1971), 75.
18. G. S. PATTERSON AND S. A. ORSZAG, *Phys. Fluids* **14** (1971), 2538.
19. H. SCHAMEL AND K. ELSÄSSER, *J. Comput. Phys.* **22** (1976), 501.
20. C. M. BENDER AND S. A. ORSZAG, "Advanced Mathematical Methods for Scientists and Engineers," McGraw–Hill, New York, 1978.
21. P. J. HANSEN AND D. R. NICHOLSON, *Amer. J. Phys.* **47** (1979), 769.
22. I. S. GRADSHTEYN AND I. M. RYZHIK, "Table of Integrals, Series, and Products," Academic Press, New York, 1980.

23. M. ABRAMOWITZ AND I. A. STEGUN, "Handbook of Mathematical Functions," Dover, New York, 1972.
24. S. G. THORNHILL AND D. TER HAAR, *Phys. Rep.* **43** (1978), 43.
25. V. G. MAKHANKOV, *Phys. Rep.* **35** (1978), 1.
26. K. E. LONNGREN, H. L. PÉCSELI, J. JUUL RASMUSSEN, AND K. THOMSEN, On the transient effects of nonlinear wave propagation in magnetized plasmas, *Phys. Scr.*, to appear.
27. V. I. KARPMAN AND E. M. MASLOV, *Zh. Eksp. Teo. Fiz.* **75** (1978), 504; *Sov. Phys.-JETP* **48** (1978), 252.
28. K. KO AND H. H. KUEHL, *Phys. Fluids* **23** (1980), 834.